ELSEVIER

PII: S0032-3861(97)00475-8

Polymer Vol. 39 No. 10, pp. 1983–1989, 1998

0032-3861/98/$19.00+0.00

Simulation of interdiffusion and its monitoring by direct energy transfer during latex film formation

K. S. Güntürk, A. T. Giz and Ö. Pekcan*
İTÜ Fen-Edebiyat Fakültesi, Maslak, İstanbul, Turkey
(Received 25 June 1996; revised 8 May 1997)

The final stage of coalescence during latex film formation was simulated by using adjacent donor and acceptor cubes. The interdiffusion of the donors and the acceptors within these cubes was generated using the Monte-Carlo technique. The delay of the donor intensity $I(t)$ by direct energy transfer (DET) was simulated for several interdiffusion steps; then the $I(t)$ curve was convolved with the experimental profile and Gaussian noise was added to generate realistic time-resolved fluorescence (TRF) data. $I(t)$ decays were fitted to the phenomenological equation to obtain the fractional mixing at each interdiffusion step. These results were compared with real TRF and steady-state fluorescence (SSF) experiments. The reliability of the Fickian diffusion model is discussed for latex film formation.

(Keywords: latex film formation; interdiffusion; mathematical modelling)

INTRODUCTION

Latex films are traditionally formed from two kinds of dispersion. One is aqueous dispersions of submicrometre colloid particles with T_g below the drying temperature, called low-T latex (soft latex)[1–3]. The second category includes aqueous and non-aqueous dispersions of colloidal particles for which T_g exceeds the drying temperature, called high-T latex (hard latex)[4]. The particles in this category of dispersion range from 0.1 to 10 μm in diameter. High- and low-T latex dispersions can be distinguished by the mature of the coalescence they have inherited. High-T latex particles remain essentially discrete and undeformed during drying, and coalescence occurs subsequently at higher temperatures, driven by healing and interdiffusion processes. Coalescence of the low-T latex particles occurs during drying and is strongly influenced by colloidal interactions in the dispersion, stabilizing surfactants and the drying process itself. In this case the particles are deformed to polyhedrons after solvent evaporation, the deformation being driven by a combination of surface and osmotic forces. Further coalescence occurs in both systems by interdiffusion of polymeric chains emanating from contiguous particles. The process of film formation is illustrated schematically in *Figure 1*.

Small-angle neutron scattering (SANS)[5] of latex films prepared from a dispersion of monodisperse spheres has shown that these films consist of ordered domains (crystallites) where the polymeric spheres are close-packed in a face-centred-cubic structure. Transmission electron microscopy (TEM) has also been used to examine the morphology of latex films[6,7]. These studies have shown that in some instances the particle boundaries disappear over time but in others the boundaries persist for months. It was suggested that in the former case the boundaries healed by polymer diffusion across the junction. In the last few years it has become possible to study latex film formation at the molecular level. SANS was used to examine deuterated particles in a protonated matrix. It was observed that the radius of the deuterated particle increases in time as the film is annealed[8], as the polymer molecules diffuse out of the space in which they were originally confined. The process of interparticle polymer diffusion has also been studied by the direct energy transfer (DET) method using transient fluorescence (TRF) measurements[1,4,9] using latex particles labelled with donor and acceptor chromophores. These studies all indicate that annealing leads to polymer diffusion and mixing as the particle junction heals during latex film formation.

Polymer diffusion obeys de Gennes scaling laws for times short compared with the tube renewal time t_{tr}, but for long times it is like a random walk process (Fickian diffusion). To be able to determine whether the diffusion is Fickian, one must compare the experimental data with the results of simulations of DET with Fickian diffusion.

Steady-state fluorescence (SSF) combined with DET was recently used to examine healing and interdiffusion processes in dye-labelled latex films[10–12].

TRF in conjunction with the DET method monitors the extent of interdiffusion of donor (D)- and acceptor (A)-labelled polymer molecules. The sample is made of a mixture of D- and A-labelled latex spheres. When this sample is annealed for a period of time and the donor fluorescence profiles are measured, each decay trace provides a snapshot of the extent of interdiffusion[4]. A film sample after annealing is considered to be composed of three regions; unmixed D, unmixed A and the mixed D-A region. This model was first empirically introduced as the two-component donor fluorescence decay[13,14]:

$$I(t) = B_1 \exp[-t/\tau_0 - C(t/\tau_0)^{1/2}] + B_2 \exp[-t/\tau_0] \quad (1)$$

where C is related to an average acceptor concentration and

* To whom correspondence should be addressed

B_1 and B_2 are the fractions of the donors which are in and out of the mixed region respectively, τ_0 is the excited-state lifetime of donors in the absence of acceptors and t is the measurement time. equation (1) has been used to fit the donor intensity decay and thereby determine B_1 and B_2, from which the diffusion coefficient is determined[3,4,13,14].

DET AND DONOR DECAY PROFILE

When donor dyes are excited using a very narrow pulse of light, the excited donor returns to the ground state either by emitting a fluorescence photon or through the non-radiative mechanism. For a well-behaved system, after exposure of the donors to a short pulse of light the fluorescence intensity decays exponentially with time. However, if acceptors are present in the vicinity of the excited donor, then there is a possibility of DET from the excited donor to the ground-state acceptors. In the classical problem of DET, neglecting back-transfer, the probability of decay of the donor r_k due to the presence of an acceptor at r_i is given by[15]:

$$P_k(t) = \exp[-t/\tau_0 - w_{ik}t] \tag{2}$$

where w_{ik} is the rate of energy transfer, given by Förster[15] as:

$$w_{ik} = \frac{3}{2}\kappa^2 \frac{1}{\tau_0}\left(\frac{R_0}{r_{ik}}\right)^6 \tag{3}$$

Here R_0 represents the critical Förster distance and κ is a dimensionless parameter related to the geometry of interacting dipoles. If the system contains N_D donors and N_A acceptors, then the donor fluorescence intensity decay can be derived from equation (3) and is given by[16]:

$$\frac{I(t)}{I(0)} = \exp(-t/\tau_0)\frac{1}{N_D}\int n_D(r_k)\,dr_k \prod_{i=1}^{N_A}\frac{1}{N_A}\int n_A(r_i)\,dr_i \exp(-w_{ik}) \tag{4}$$

Here n_D and n_A represent the distribution functions of donors and acceptors. In the thermodynamic limit equation (4) becomes[16]:

$$\frac{I(t)}{I(0)} = \exp(-t/\tau_0)\frac{1}{N_D}\int n_D(r_k)\,dr_k \exp\left(-\int n_A(r_i)\,dr_i\,[1-\exp(-w_{ik}t)]\right) \tag{5}$$

This equation can be used to generate donor decay profiles by Monte-Carlo techniques. It is shown that the equation (4) also leads to equation (1), which can be compared with the experimental data[3]. The argument is summarized below for clarity. Changing to the coordinate $r_{ik} = r_i - r_k$ leads to:

$$\frac{I(t)}{I(0)} = \exp(-t/\tau_0)\frac{1}{N_D}\int n_D(r_k)\,dr_k \times \prod_{i=1}^{N_A}\int_{r_K}^{R_g - r_K} n_A(r_{ik}+r_K)\,dr_{ik}\exp(-w_{ik}t) \tag{6}$$

where R_g is an arbitrary upper limit. Placing a particular donor at the origin and assuming that the mixed and unmixed regions are created during interdiffusion of D and A, equation (6) becomes:

$$\frac{I(t)}{I(0)} = f_I \exp(-t/\tau_0)\prod_{i=1}^{N_A}\frac{1}{N_A}\int_0^{R_g} n_A(r_{ik})\,dr_{ik} \exp(-w_{ik}t) + f_{II}\exp(-t/\tau_0) \tag{7}$$

where

$$f_{I,II} = \frac{1}{N_D}\int_{I,II} n_D(r_k)\,dr(k) \tag{8}$$

represent the fractions of donors in the mixed (I) and unmixed (II) regions respectively. The integral in equation (7) produces a Förster type of function[17,18]:

$$\prod_{i=1}^{N_A}\frac{1}{N_A}\int_0^{R_g} n_A(r_{ik})\,dr_{ik}\exp(-w_{ik}t) = \exp[-C(t/\tau_0)^{1/2}] \tag{9}$$

where C is proportional to the acceptor concentration. Then equation (7) becomes identical to equation (1) as:

$$\frac{I(t)}{I(0)} = f_I \exp[-t/\tau_0 - C(t/\tau_0)^{1/2}] + f_{II}\exp(-t/\tau_0) \tag{10}$$

where f_I and f_{II} correspond to B_1 and B_2 in equation (2). Here it is useful to define the mixing ratio K representing the order of mixing during interdiffusion of the donors and the acceptors as:

$$K = \frac{B_1}{B_1 + B_2} = \frac{f_I}{f_I + f_{II}} \tag{11}$$

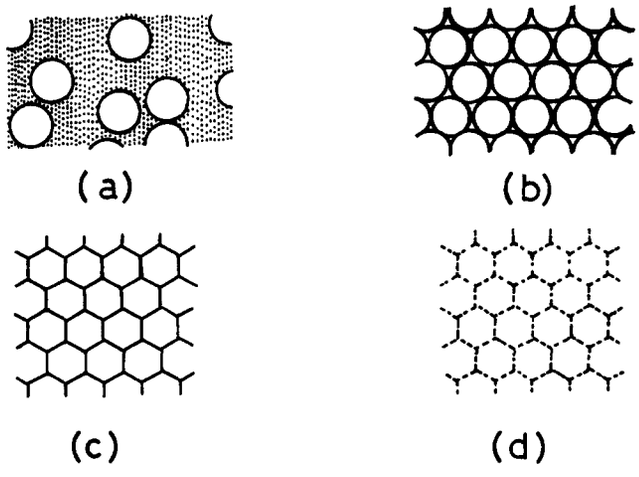

Figure 1 Stages during the process of film formation from soft latex particles: (a) latex dispersion; (b) dense packing of particles; (c) deformation of particles and beginning of coalescence; (d) further coalescence by interdiffusion of chains. Note that stage (c) does not take place during film formation from hard latex particles

SIMULATION OF DONOR DECAY IN A CUBIC LATTICE

In this work we try to simulate the interdiffusion of donors and acceptors between two adjacent cubes using the Monte-Carlo technique. This simulation corresponds to the last stage of coalescence during the latex film formation process. Here we have simplified the process by using cubes instead of the polyhedrons. Donors and acceptors are randomly distributed in separate adjacent cubes, then Brownian motion of these particles is generated for several

interdiffusion steps and the decay of the donor intensity by DET is simulated for the configurations at the end of each step. The D intensity $I(t)$ curve is convolved with the experimental lamp profile and Gaussian noise is added to generate realistic TRF data. B_1 and B_2 values are determined by fitting the simulated data to equation (1) using non-linear least squares analysis. These results are compared with those of TRF and SSF experiments in the last part of this paper.

Donor and acceptor dots are randomly distributed in separate adjacent cubes. The side of the cubes is taken as 100 Å and the Förster distance as 26 Å. $N_D = 200$ donor and $N_A = 200$ acceptor sites are used. The diffusion is simulated by a random walk of the donors and acceptors. Reflecting boundary conditions are used in the sides of the cubes except at the interface of the donor and acceptor cubes,

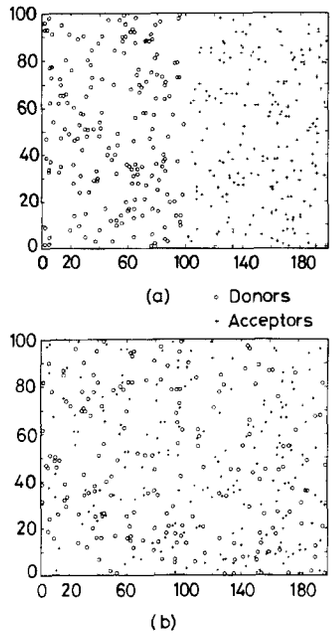

Figure 2 Randomly diatributed donors and acceptors in adjacent cubes, (a) before and (b) after interdiffusion

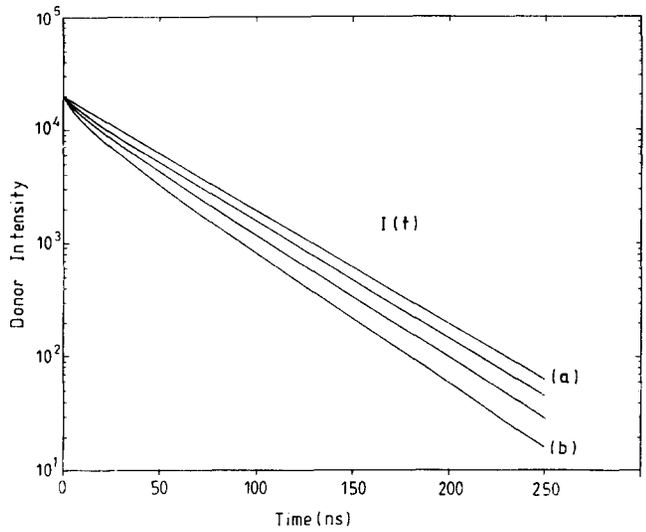

Figure 3 Donor decay profiles for various interdiffusion steps. (a) and (b) correspond to steps shown in *Figure 2*(a) and (b) respectively. (Sizes are adjusted for presentation)

where the donors and acceptors are allowed to cross over into the adjacent cube to generate interdiffusion. *Figure 2* shows the placement of the donors and acceptors before and after the interdiffusion step. The w_{ik} values for each donor acceptor pair are obtained from equation (3). The parameter κ^2 is chosen as 0.476, a value appropriate for immobile dyes[19], and the donor lifetime τ_0 is taken as 44 ns. equation (5) is then used to simulate the donor intensity $I(t)$ decay profiles. $I(0) = 2 \times 10^4$ is chosen and the decay profiles are obtained for a 250 ns period divided into 250 channels of 1 ns each. *Figure 3* presents donor decay profiles for various interdiffusion steps. (The values of the Förster distance and donor lifetime as above are appropriate for phenanthrene donors in the presence of anthracene acceptors.)

In real TRF experiments the fluorescence decay measurements are made by the single photon counting (SPC) technique, where the experimentally obtained decay $\phi(t)$ is obtained by convolution of $I(t)$ with the instrument response from the lamp $L(t)$:

$$\phi(t) = \int_0^t L(t)I(t-s)\,\mathrm{d}s \qquad (12)$$

In typical SPC experiments[3,4] using phenanthrene donors, 2,5-bis(5-*tert*-butyl-2-benzoxazotyl)thiophene (BBOT) in ethanol is used as a standard for $L(t)$. Here we choose the experimentally obtained response function of BBOT, which has a lifetime of 1.1 ns, and convolve it with $I(t)$ to obtain $\phi(t)$ intensities from equation (12). The $L(t)$ response

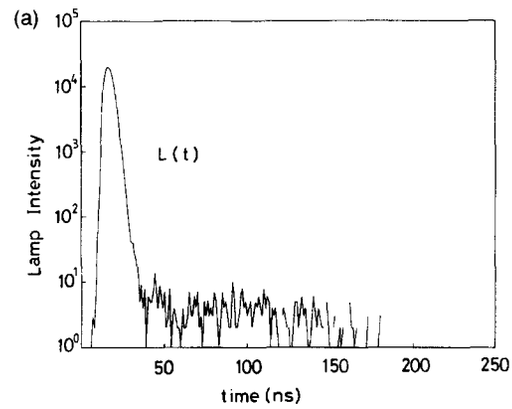

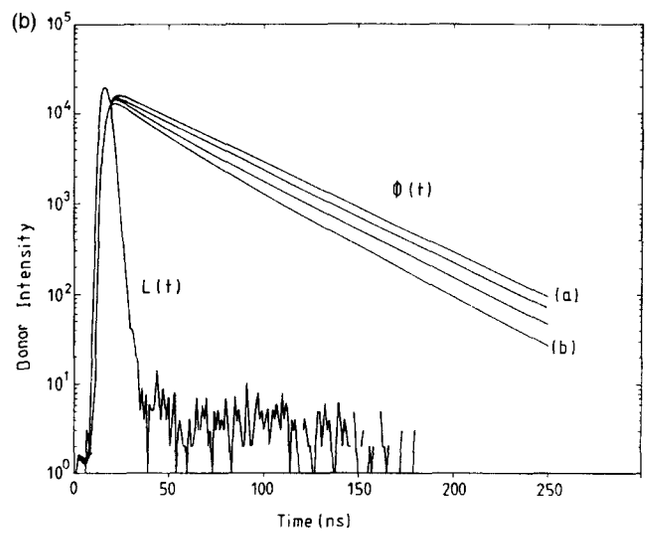

Figure 4 (a) Experimental response function $L(t)$. (b) Convoluted donor decay profiles $\phi(t)$ obtained from the data in *Figure 3* using equation (12)

function and the $\phi(t)$ decay profiles obtained from the data in *Figure 3* are shown in *Figure 4(a)* and *(b)* respectively. After convolution, Gaussian noise generated by the Box *et al.* algorithm[20] is added to the $\phi(t)$ curves in *Figure 4(b)*. The noisy data profiles are presented in *Figure 5* for the data in *Figure 3*.

To test how realistic are the simulated donor intensity curves, the B_1 and B_2 parameters representing the degree of mixing in equation (1) must be compared with the values obtained by counting the donors in the mixed and unmixed regions. The simulated data in *Figure 5* are fitted by non-linear least squares (NLLS) analysis to produce the B_1 and B_2 values[21]. In fitting the model, a fixed value of C is chosen from the most mixed sample (b) and this value is used in all the runs[21]. The mixing ratio K is calculated from equation (11) for each interdiffusion step and plotted versus time in *Figure 6*.

The degree of mixing can also be obtained by a combinatorial method which divides the whole region inside the cube into m equal parts. Then the following relations can be used to obtain the mixing ratio K':

$$S = \sum_{i=1}^{m} \left[\left(N_{D_i} - \frac{N_D}{m} \right)^2 + \left(N_{A_i} - \frac{N_A}{m} \right)^2 \right] \quad (13)$$

$$K' = 1 - \frac{S}{S_{max}} \quad (14)$$

Here N_{D_i} and N_{A_i} are the numbers of donors and acceptors located in the ith region. K' is represented by the solid line in *Figure 6*, which shows good agreement with the K values obtained by the fitting procedure.

To test whether the simulated interdiffusion is Fickian or not, the planar sheet model is chosen[22]. In this model the fraction of the diffusing substance that has diffused out of the planar sheet at time t is given by:

$$K_s = \frac{8}{\pi} \sum_{n=0} \frac{1}{(2n+1)^2} \exp\left(- \frac{D(2n+1)^2 \pi^2 t}{a^2} \right) \quad (15)$$

where D is the diffusion coefficient and a is the maximum distance over which diffusion can occur. Since $\lim_{t \to \infty} K_s = 1$, equation (15) can be written for $n = 0$ in the form:

$$\ln(1 - K_s) = - \frac{D\pi^2 t}{a^2} \quad (16)$$

It is seen from *Figure 6* that the behaviour of the simulated data predicts Fickian model; however, to test the realization, ln(1-K) values are plotted versus time in *Figure 7* and are fitted to equation (16). In *Figure 7* the solid line is the fitting curve and the dots represent the data.

The results are successful except in the early time region, that is, < 30% mixing fraction. The failure at early times cannot indicate that at such times the diffusion has not yet acquired a Fickian character. The simulation is a random walk. Here it has to be noted that for both the TRF and SSF experiments, equation (1) is applicable only to measurements made at times much longer than the tube renewal time. There are several reasons for this. At times short compared with the tube renewal time, the diffusion is expected not to be a random walk but to obey de Gennes's law. In the first time steps, a random walk does not obey the Fickian model and finally the Fickian model does not lead to equation (1)[23,24]. However, at times long compared with the tube renewal time these objections are no longer valid.

From this we suggest that for realistic TRF and SSF experiments, care must be taken in speculating on the nature of the diffusion based on the results at early times.

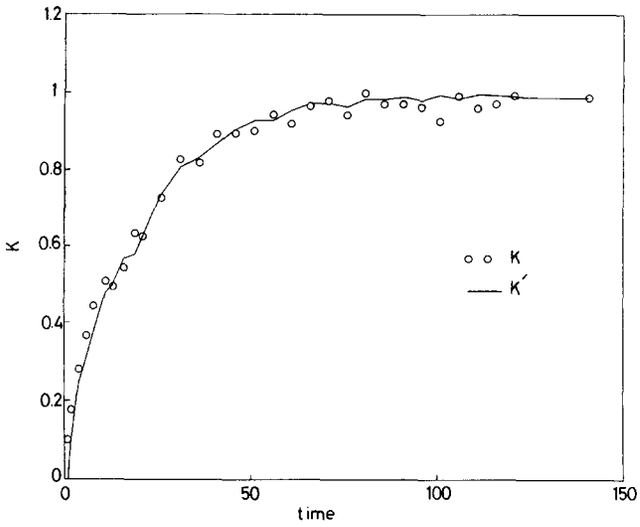

Figure 6 Mixing ratio K obtained from equation (11) versus time. The solid line represents the mixing ratio K' produced by combinatorial method using equation (14)

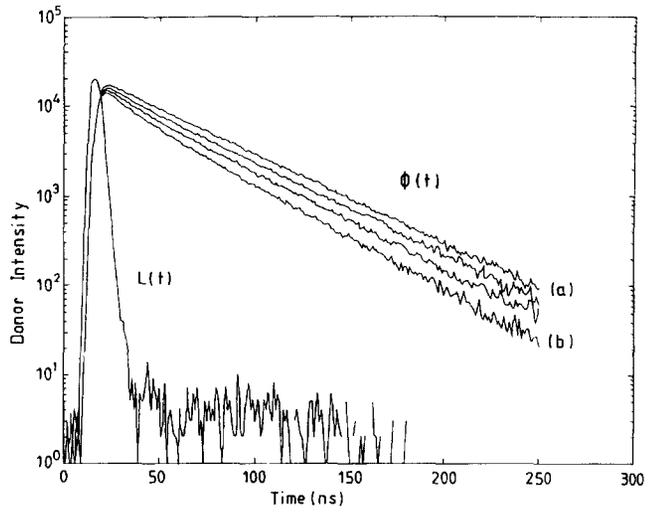

Figure 5 Noisy donor decay profile obtained from the data in *Figure 4*(b) by adding a Gaussian noise

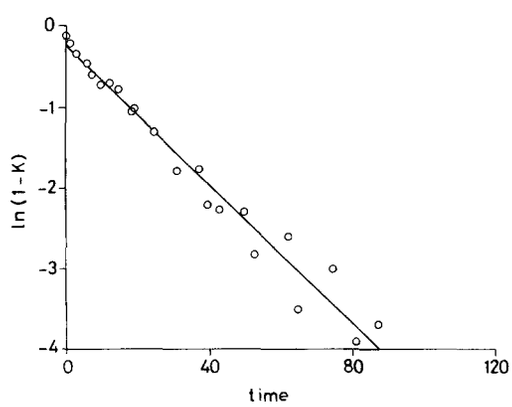

Figure 7 Plot of the data of *Figure 6* in logarithmic form versus time. The solid line is the fitting curve ln(1-K_s) from equation (16)

INTERDIFFUSION EXPERIMENTS

This section presents some results of TRF and SSF experiments for comparison with the simulated data. Then the reliability of the Fickian model is discussed to interpret the experimental results.

Transient fluorescence (TRF) experiments:

High-T poly(methyl methacrylate) (PMMA) latex particles labelled with phenanthrene (Phe) donors and anthracene (An) acceptors were used for TRF experiments[4,13]. These particles were prepared by non-aqueous dispersion polymerization[25] and thoroughly characterized by several DET experiments[26,27]. Phe- and An-labelled 1 μm diameter particles have two components. The major component, PMMA, forms 96% of the material. The remaining 4% is polyisobutylene (PIB), which forms an interpenetrating network through the particle interior[28,29].

For polymer interdiffusion experiments, equal amounts of Phe- and An-labelled particles were dispersed in pentane, which was then evaporated to form a hard latex film on the inner surface of a quartz tube. This film was then annealed above the glass transition temperature (T_g) of PMMA for various periods at 150 and 160°C. Fluorescence decay measurements were carried out by the time-correlated single photon counting technique, using a pulsed lamp source. Samples were excited at 295 nm and emission was detected at 345 nm. Data were collected over three decades of decay and fitted by non-linear least squares with BBOT in ethanol as a standard to obtain B_1 and B_2 from equation (1); $\tau_0 =$ 44 ns was chosen and C was kept constant during the fitting procedure. The experimental mixing ratios K are plotted versus time in *Figure 8*, which predicts a Fickian diffusion model. Plots of ln(1-K) versus time are presented in *Figure 9(a)* and *(b)* for the annealing temperatures of 150 and 160°C respectively. The data in *Figure 9* were fitted to equation (16) for each temperature and D values were obtianed from the slopes of the linear curves, equal to 4.08×10^{-13} and 4.83×10^{-13} cm^{2}s^{-1} respectively. These values are quite reasonable for a polymer chain diffusing above T_g during latex film formation from high-T particles. Similar values have been reported with different experimental techniques[30–33].

Steady-state fluorescence (SSF) experiments

Prager and Tirrel[34] studied interdiffusion of a polymer chain in terms of the SSF of an acceptor emission intensity $I_A(t)$ due to DET from a donor. $I_A(t)$ is proportional to the quantum efficiency $E(t)$ of energy transfer, which is in turn proportional to the integrated D and A pair distribution

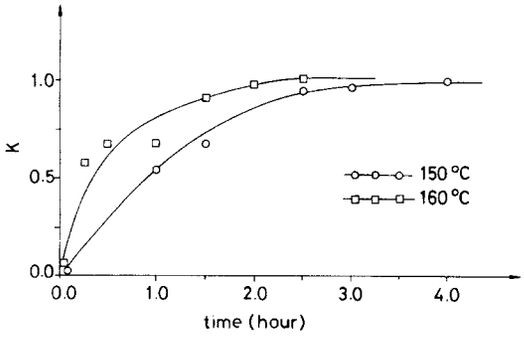

Figure 8 Mixing ratio K versus time obtained from interdiffusion experiments using Phe and An labelled particles at 150 and 160°C annealing temperatures

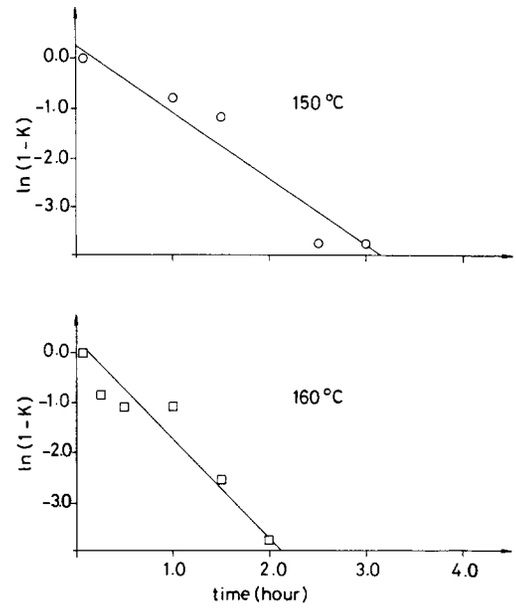

Figure 9 Plots of ln(1-K) versus time for the data of *Figure 8*. The solid lines show the fitting curves obtained from equation (16)

function. This integrated area evolves due to interdiffusion which corresponds to the mixed region of D and A pairs. If the x-axis is normal to the planar interface, then the acceptor intensity can be written as:

$$I_A(t) - I_A(0) = I_0 \alpha \int_{-\infty}^{\infty} C(x,t)[C_0 - C(x,t)]\,dx \qquad (17)$$

where $I_A(0)$ is the acceptor emission intensity at $t = 0$, I_0 is the incident light intensity and α is a constant; $C(x,t)$ is the concentration profile of acceptors at time t and C_0 is its value at the interface.

At times longer than the tube renewal time T_r[35], concentration profiles can be obtained from Fick's diffusion law[21] and equation (17) can be written for the planar sheet as:

$$\frac{I_A(t) - I_A(0)}{I_A(\infty) - I_A(0)} = \frac{(Dt)^{1/2}}{a} \qquad (18)$$

where D is the centre-of-mass diffusion coefficient of the polymer chains, a is the thickness of the planar sheet and $I_A(\infty)$ represents the value of $I_A(t)$ as t approaches ∞. Alternatively, one can use the decrease in donor emission intensity $I_D(t)$ as a measure of the energy transfer in the mixed region:

$$\frac{I_D(t) - I_D(0)}{I_D(\infty) - I_D(0)} = \frac{(Dt)^{1/2}}{a} \qquad (19)$$

If the optical density of the film sample is constant throughout the SSF measurements, equation (19) can be expressed in terms of energy transfer efficiency as[3]:

$$\frac{E(t)}{E(\infty)} = \frac{(Dt)^{1/2}}{a} \qquad (20)$$

Using the donor decay model equation (10), it can be shown that the fraction of donors in the mixed region can

be written as[3]:

$$B_1 = \frac{(Dt)^{1/2}}{a} \tag{21}$$

A combination of equations (18)–(21) can be used to study polymer interdiffusion by the SSF technique. Hard latex films were prepared from PMMA particles labelled with naphthalene (N) donors and pyrene (P) acceptors and annealed for various periods above T_g at 180°C. These particles were similar to those described in the previous subsection. The latex film sample was excited at 286 nm and N and P spectra were observed between 300 and 500 nm by a spectrofluorimeter. N and P intensities, corrected for optical density variations, are plotted versus time in *Figure 10*, where it can be seen that the decrease in N intensity $I_N(t)$ corresponds to an increase in P intensity $I_P(t)$[36,37]. Equations (18) and (19) can be used to obtain D values by fitting them to the data in *Figure 10(a)* and *(b)* respectively. *Figure 11* shows the goodness of the fits. The D values are 1.4×10^{-13} and 1.5×10^{-13} cm^2s^{-1} respectively. These values are slightly smaller than those obtained by the TRF experiments. We do not think that this difference is model-dependent. It is probably caused by the difference in the molecular weights of the polymers used in the two experiments, which were 2.5×10^5 and 1.5×10^5 in the SSF and the TRF experiments respectively. In both experiments the chains carrying the donor and acceptor labels were of comparable length.

In conclusion, this work has shown that chain interdiffusion during film formation from high-T latex particles obeys a Fickian model for planar sheets.

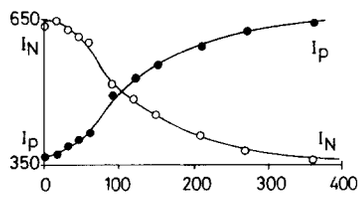

Figure 10 Plots of (a) naphthalene (N) and (b) pyrene (P) intensity variations versus time during film formation from N- and P-labelled PMMA particles at 180°C annealing temperature. $I_N(t)$ and $I_P(t)$ were obtained after optical density corrections

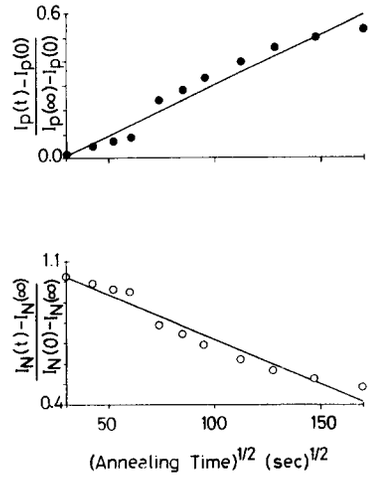

Figure 11 Plot of the data of *Figure 10* using equations (19) and (18) respectively. The solid lines are the fitting curves

Using equation (1) to interpret the TRF experiments is unsuccessful at times $< 30\%$ mixing ratio but quite reliable beyond this point. The main difficulty in the SSF experiment arises from the optical density correction[11,12,35] and can be overcome by using direct fluorescence measurements in parallel with the DET experiment during latex film formation. Both the TRF and SSF techniques study chain diffusion at the molecular level and we believe both produce reliable D values.

If the molecular weights of the D- and A-labelled chains are different or if these chains are not monodisperse, then different chain lengths will give different diffusion time scales. The resulting random walk will not be a single Fickian but a superposition of Fickian diffusions.

ACKNOWLEDGEMENTS

We thank Prof. M.A. Winnik for supplying the materials, and Prof. A. Erzan for helpful discussions.

REFERENCES

1. Winnik, M. A., Wang, Y. and Haley, F., *J. Coat. Technol.*, 1952, **64**, 51.
2. Wang, Y., Kats, A., Juhne, D., Winnik, M. A., Shivers, R. R. and Dinsdalw, C. J., *Langmuir*, 1992, **8**, 1435.
3. Wang, Y., Zhao, C. L. and Winnik, M. A., *J. Chem. Phys.*, 1991, **95**, 2143.
4. Pekcan, Ö.. Winnik, M. A. and Croucher, M. D., *Macromolecules*, 1990, **23**, 2673.
5. Rieger, J., Dipper, O., Hädricke, E. and Ley, G., in *Colloidal Polymer Particles*, ed. J. W. Goodwin and R. Bascall. Academic Press, London, 1995.
6. Vanderhof, J.W., *Br. Polym. J.*, 1970, **2**, 161.
7. Distler, D. and Kanig, G., *Colloid Polym. Sci.*, 1978, **256**, 1052.
8. Hahn, K., Ley, G., Schuller, H. and Oberthur, R., *Colloid Polym. Sci.*, 1988, **66**, 631.
9. Zhao, C. L., Wang, Y., Hruska, Z. and Winnik, M. A., *Macromolecules*, 1990, **23**, 4082.
10. Canpolat, M. and Pekcan, Ö., *J. Polym. Sci., Polym. Phys. Ed.*, 1996, **34**, 691.
11. Canpolat, M. and Pekcan, Ö., *Polymer*, 1995, **36**, 2025.
12. Canpolat, M. and Pekcan, Ö., *Polymer*, 1995, **36**, 4433.
13. Winnik, M. A., Pekcan, Ö. and Croucher, M. D., in *Scientific Methods for the Study of Polymer Colloids and their Applications*, ed. F. Condon and R. H. Otterwell. NATO ASI Series, Kluwer, 1988.
14. Wang, Y. and Winnik, M. A., *Macromolecules*, 1993, **26**, 3147.
15. Förster, T. H., *Ann. Phys.*, 1948, **2**, 55.
16. Frederickson, G. H., *Macromolecules*, 1986, **19**, 441.
17. Klafter, J. and Blumen, A., *J. Chem. Phys.*, 1984, **80**, 875.
18. Bauman, J. and Fayer, M. D., *J. Chem. Phys.*, 1986, **85**, 408.
19. Lakowicz, J. R., in *Principles of Florescence Spectroscopy*. Plenum Press, New York, 1983.
20. Demas, J. N., *Excited State Lifetime Measurements*. Academic Press, New York, 1983.
21. Güntürk, K. S., Giz, A. T. and Pekcan, Ö., *Eur. Polym. J.* (in press).
22. Crank, J., *The Mathematics of Diffusion*. Clarendon Press, Oxford, 1975.
23. Farinha, J. P. S., Martinho, J. M. G., Yekta, A. and Winnik, M. A., *Macromolecules*, 1995, **28**, 6084.
24. Farinha, J. P. S., Martinho, J. M. G., Kawaguchi, S., Yekta, A. and Winnik, M. A., *J. Chem. Phys.*, 1996, **100**, 12552.
25. Pekcan, Ö., Egan, L. S., Winnik, M. A. and Croucher, M. D., *Macromolecules*, 1990, **23**, 2210.
26. Pekcan, Ö., Winnik, M. A. and Croucher, M. D., *J. Colloid Interface Sci.*, 1983, **95**, 420.
27. Pekcan, Ö., Winnik, M. A. and Croucher, M. D., *Phys. Rev. Lett.*, 1988, **61**, 641.
28. Pekcan, Ö., *Chem. Phys. Lett.*, 1992, **20**, 198.
29. Pekcan, Ö., *Chem. Phys.*, 1993, **177**, 619.
30. Hahn, K., Ley, G., Schuller, H. and Oberthur, R., *Colloid Polym. Sci.*, 1986, **264**, 1029.
31. Hahn, K., Ley, G. and Oberthur, R., *Colloid Polym. Sci.*, 1988, **266**, 631.

32. Linne, M.A., Klein, A., Miller, G.A., Sperling, L.H. and Wignall, G.D., *J. Macromol. Sci. Phys. B*, 1988, **27**, 217.
33. Yoo, Y. N., Sperling, L. H., Glinka, C. J. and Klein, A., *Macromolecules*, 1990, **23**, 4624.
34. Prager, S. and Tirrell, M., *J. Chem. Phys.*, 1981, **75**, 5194.
35. De Gennes, P. G., *J. Chem. Phys.*, 1971, **75**, 572.
36. Pekcan, Ö. and Canpolat, M., *Polymer* (in press).
37. Pekcan, Ö. and Canpolat, M., in *Film Formation in Waterborne Coatings*, ed. T. Provder, M. A. Winnik and M. W. Urban. Symposium Series 648, American Chemical Society, Washington, DC, 1996.